



TITLE:

# Evaluation of magnetic properties in ferromagnetic martensite particle using type 304 stainless steel wire

AUTHOR(S):

Kinoshita, K.

---

CITATION:

Kinoshita, K.. Evaluation of magnetic properties in ferromagnetic martensite particle using type 304 stainless steel wire. AIP Advances 2020, 10: 015313.

ISSUE DATE:

2020-01-01

URL:

<http://hdl.handle.net/2433/255563>

RIGHT:

All article content, except where otherwise noted, is licensed under a Creative Commons Attribution (CC BY) license (<http://creativecommons.org/licenses/by/4.0/>).

# Evaluation of magnetic properties in ferromagnetic martensite particle using type 304 stainless steel wire

Cite as: AIP Advances **10**, 015313 (2020); <https://doi.org/10.1063/1.5131048>

Submitted: 09 October 2019 . Accepted: 07 December 2019 . Published Online: 08 January 2020

K. Kinoshita

## COLLECTIONS

Paper published as part of the special topic on [Chemical Physics](#), [Energy, Fluids and Plasmas](#), [Materials Science](#) and [Mathematical Physics](#)



View Online



Export Citation



CrossMark

## ARTICLES YOU MAY BE INTERESTED IN

[Magnetic dilution by severe plastic deformation](#)

AIP Advances **10**, 015210 (2020); <https://doi.org/10.1063/1.5128058>

[Thermal annealing induced enhancement of room temperature magnetic memory effect in Fe-doped NiO nanoparticles](#)

AIP Advances **10**, 015211 (2020); <https://doi.org/10.1063/1.5129785>

[Determination of demagnetizing factors using first-order reversal curves and ferromagnetic resonance](#)

AIP Advances **10**, 015318 (2020); <https://doi.org/10.1063/1.5129969>

AIP Advances Nanoscience Collection

READ NOW!

# Evaluation of magnetic properties in ferromagnetic martensite particle using type 304 stainless steel wire

Cite as: AIP Advances 10, 015313 (2020); doi: 10.1063/1.5131048

Presented: 5 November 2019 • Submitted: 9 October 2019 •

Accepted: 7 December 2019 • Published Online: 8 January 2020



View Online



Export Citation



CrossMark

K. Kinoshita<sup>a)</sup>

## AFFILIATIONS

Department of Energy Conversion Science, Graduate School of Energy Science, Kyoto University, Yoshida-honmachi, Sakyo-ku, Kyoto 606-8501, Japan

**Note:** This paper was presented at the 64th Annual Conference on Magnetism and Magnetic Materials.

<sup>a)</sup>Correspondence e-mail: [kinosita@energy.kyoto-u.ac.jp](mailto:kinosita@energy.kyoto-u.ac.jp)

## ABSTRACT

In this study, the magnetic properties of a single martensite particle were investigated using type 304 stainless wire, which can reduce the number of crystal grains per unit area. First, the magnetization curve of wire specimens with different martensite fractions was measured by a SQUID magnetic flux meter. Then, the coercivity and susceptibility parameters were evaluated from the magnetization curve and factors contributing to these parameters were discussed. It was found that the coercivity values along the long and short axes of wire specimens with a diameter of 0.4 mm increased and subsequently decreased with an increase in the martensite fraction. Further, the susceptibility values of the same specimen along the long axis increased and along the short axis decreased with increasing martensite fractions. The results indicate that the coercivity and susceptibility of a martensite particle are affected by the size of variant clusters and the shape anisotropy of the martensite particle.

© 2020 Author(s). All article content, except where otherwise noted, is licensed under a Creative Commons Attribution (CC BY) license (<http://creativecommons.org/licenses/by/4.0/>). <https://doi.org/10.1063/1.5131048>

## I. INTRODUCTION

Austenitic stainless steel, including type 304 stainless steel (SUS304), is an interesting magnetic composite material due to the ferromagnetic martensite particles generated by plastic deformation. We have developed a fatigue sensor by applying that unique property and need a magnetic model to design the sensor.<sup>1</sup> Therefore, we previously derived a magnetic composite model incorporating the aspect ratio and the orientation distribution of martensite particles and showed that it can provide a qualitative basis as to how permeability varies with martensite fraction.<sup>2</sup> However, the theoretical results did not quantitatively agree with the experimental results. Miura *et al.*<sup>3</sup> showed that the coercivity of SUS304 first increased and subsequently decreased with increasing martensite fraction. This is consistent with the dependence of coercivity on the grain size of the nanocrystalline materials.<sup>4</sup> Their result suggests that the dichotomy between the experimental and theoretical results may be resolved by factoring in the possibility that the

magnetization curve of a single martensite particle may vary with its size and morphology. However, to our knowledge, the magnetization curve for a single martensite particle has not been investigated because of difficulty in measuring it. Moreover, little is known about the relationship between the magnetic properties and the internal structure of a martensite particle. The martensite phase generates the TRIP effect, which is a phenomenon for developing strength and ductility in SUS304.<sup>5</sup> Because the strength of the martensite phase is important for this effect and is controlled by the internal structure, the evaluation by magnetic measurement is useful for plastic working.

This study was conducted with the objective of reducing the effect of the heterogeneous distribution of martensite particles on the magnetization curve by decreasing the number of crystal grains per unit area using SUS304 wires. To this end, the magnetization curve of the SUS304 wires was measured with different martensite fractions by using a SQUID magnetic flux meter and evaluated the magnetic properties, including coercivity and susceptibility,

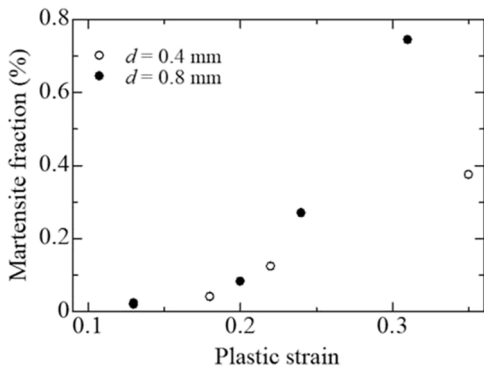


FIG. 1. Relationship between plastic strain and martensite fraction.

were investigated. In addition, major factors contributing to their dependency on the martensite fraction were discussed.

## II. EXPERIMENTAL METHOD

The specimens used were commercial SUS304 wires with diameters of 0.4 mm and 0.8 mm respectively. Following solution treatment at 1293 K for 3 h, specimens with specific martensite fractions were prepared by applying tensile stresses of 550, 600, 650 and 700 MPa using a tensile test machine (AGS-500NG, SHIMADZU Inc). The crystal grain sizes post solution treatment were 37 and 46  $\mu\text{m}$  respectively. The diameters of the specimens were decided in reference to Fukumaru et al.<sup>6</sup> to be able to sustain a tensile strain of more than 20%. Plastic strain was determined by measuring the distance between marking lines using an optical microscope. The magnetization curve was measured in the long (L)-axis and short (S)-axis directions using a SQUID magnetic flux meter (MPMS-5S, Quantum Design Inc). The martensite fraction was evaluated using a saturation magnetization method<sup>7</sup> at the saturation magnetization of 100% martensite phase of 154 emu/g.<sup>8</sup> Before evaluating the coercivity  $H_c$  and susceptibility  $\chi$ , the magnetization was divided by the martensite fraction to normalize the magnetization value. The  $H_c$  was evaluated by using a spline interpolation for a normalized magnetization curve. Using a mean magnetization curve, the susceptibility  $\chi_0$  was

evaluated via the linear approximation method for that curve near the origin.

## III. EXPERIMENTAL RESULT

### A. Martensite fraction

Fig. 1 shows the relationship between martensite fraction  $V_f$  and plastic strain. When plastic strain exceeds 0.2, the  $V_f$  of the specimen with diameter 0.8 mm (Specimen D8) exponentially increases in a manner consistent with previous results.<sup>5</sup> Conversely, the  $V_f$  of the specimen with diameter 0.4 mm (Specimen D4) displays a linear increment under the same conditions. The parameter  $\beta$ , defined as an emerging probability of  $\alpha'$  martensite nucleus in a shear band crossing, is obtained using Eq. (1) of the OC model.<sup>5</sup> The  $\beta$  value was calculated to be 3.7, whereas that of Specimen D4 was significantly smaller at 0.081. As the  $\beta$  of the specimen is small, the number of particles does not increase significantly as it is difficult to generate new particles in this specimen. This indicates that the preliminary objective was achieved.

$$V_f = 1 - \exp\{-\beta[1 - \exp(-\alpha\varepsilon_p)]^n\}. \quad (1)$$

where,  $\alpha$ ,  $\beta$  and  $n$  are material parameters.  $\varepsilon_p$  is the equivalent plastic strain.

### B. Coercivity

Figs. 2(a) and (b) show the relationship between coercivity  $H_c$  and martensite fraction  $V_f$  in the L- and S-axis respectively. Although  $H_c$  along the L-axis ( $H_c^L$ ) of Specimen D8 decreased with increasing  $V_f$ , that of Specimen D4 increased from  $V_f = 0.02\%$  to  $V_f = 0.041\%$ , and then decreased with increasing  $V_f$ . On the other hand,  $H_c$  along the S-axis ( $H_c^S$ ) of both specimens increased and then decreased with increasing  $V_f$ . Notably, whereas the  $H_c$  of Fe with the crystal grain size of 20 nm is approximately 40 A/cm,<sup>9</sup> all of the  $H_c$  values obtained in this study were an order of magnitude greater.

### C. Susceptibility

Figs. 3(a) and (b) show the relationship between the susceptibility near the origin  $\chi_0$  and martensite fraction  $V_f$  in the L- and S-axis,

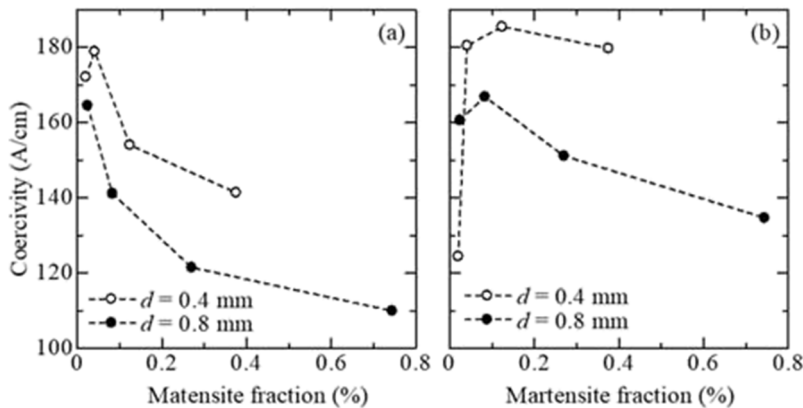


FIG. 2. Relationship between coercivity and martensite fraction in (a) the L-axis direction and (b) S-axis direction.

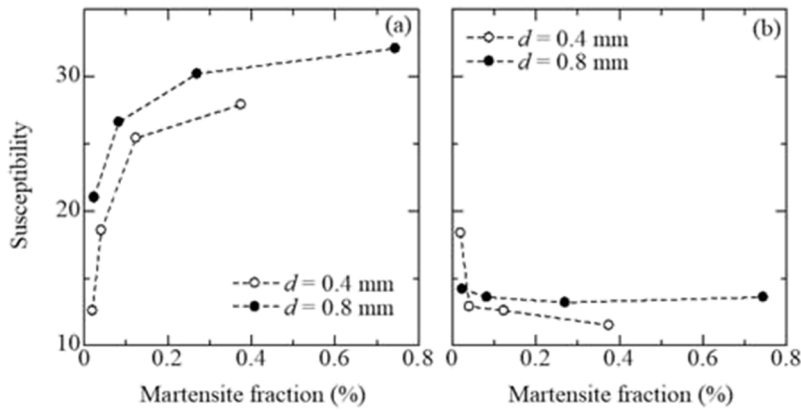


FIG. 3. Relationship between susceptibility and martensite fraction in (a) the L-axis direction and (b) S-axis direction.

respectively. The susceptibility near the origin along the L-axis ( $\chi_o^L$ ) of both specimens show a significant increase with increasing  $V_f$  followed by a slower rise with increasing  $V_f$ . In contrast, the susceptibility near the origin along the S-axis ( $\chi_o^S$ ) of both specimens show a tendency to decrease with increasing  $V_f$ . The magnitude of  $\chi_o^L$  and  $\chi_o^S$  was three orders of magnitude greater than that of the initial susceptibility converted from the initial permeability of Fe based alloy at a grain size of 20 nm.<sup>10</sup>

#### IV. DISCUSSION

##### A. Predominant factors of coercivity

The predominant factors of  $H_c$  for fine ferromagnetic powders have been previously shown to include internal stress, inclusion, dislocation, grain size, shape anisotropy, and interparticle interaction.<sup>11</sup> This study focuses primarily on the grain size, dislocation and shape anisotropy as major factors for the  $H_c$  of martensite particles. Internal stress and interparticle interaction were excluded in this current study because of the complications associated with quantifying their effects on  $H_c$ . Such quantification is difficult for internal stress because the sign and value distributions are inconsistent in a martensite particle.<sup>12</sup> Numerical analysis is needed to quantitatively estimate the effect of interparticle interaction on  $H_c$ .

##### 1. Grain size

Herzer<sup>4</sup> suggested that the coercivity of nanocrystalline materials increases and then decreases with increasing grain size owing to the relationship between grain size and exchange length  $L_{ex}$ . However, under theoretical conditions, random orientation of each crystal grain is required. Because the martensite particles of SUS304 are composed of fine multiple variants,<sup>12</sup> they can be assumed to be fine crystal grains with random orientation. When  $L_{ex}$  is greater than the fine crystal grain size  $D$ , the  $H_c$  increases in a manner proportional to  $D^6$ , as shown in Eq. (2).<sup>4</sup> Conversely, when  $L_{ex}$  is smaller than the fine crystal grain size  $D$ , the  $H_c$  decreases in a manner inversely proportional to  $D$ , as shown in Eq. (3).<sup>4</sup>

$$H_c = p_c^1 \frac{K_1^4 D^6}{M_s A^3}, \quad L_{ex} > D. \quad (2)$$

$$H_c = p_c^2 \frac{\sqrt{A K_1}}{M_s D}, \quad L_{ex} < D. \quad (3)$$

where  $A$  is the exchange stiffness,  $K_1$  is the magneto crystalline anisotropy, and  $p_c^1$  and  $p_c^2$  are material constants.  $p_c^1 = 0.64$  for cubic particles and  $p_c^2 = 4.4$  for BCC phase.<sup>9</sup> Fig. 4 shows the relationship between the measured  $H_c$  and calculated  $D$  obtained using the measured  $H_c$  and Eq. (3) in the case of increased  $H_c$ , or Eq. (4) in the case of the decreased  $H_c$ . Because  $A$  and  $K_1$  of the martensite phase of SUS304 have not been reported, Fe data ( $A = 2.0 \times 10^{-11} \text{ J/m}$ ,  $K_1 = 5.0 \times 10^4 \text{ J/m}^3$ )<sup>9</sup> were used to calculate the  $D$  values. The  $D$  values were approximately 20 nm in the range of increasing  $H_c$  and 40–60 nm in the range of decreasing  $H_c$ . The size of fine variant was approximated to be one hundred nanometers from our analysis of the EBSD picture.<sup>12</sup> However, the size of the martensite particles of their specimen was greater than 100  $\mu\text{m}$ , which is considerably greater than the crystal grain size of the specimens used in this study. Because it is not greater than the crystal grain size, the size of the variant cluster of the specimens in this study would therefore be smaller than that of their specimens. Moreover, it has been shown that the variant size increases with increasing martensite particle size.<sup>13</sup> Therefore, the variant size can potentially influence the  $H_c$ .

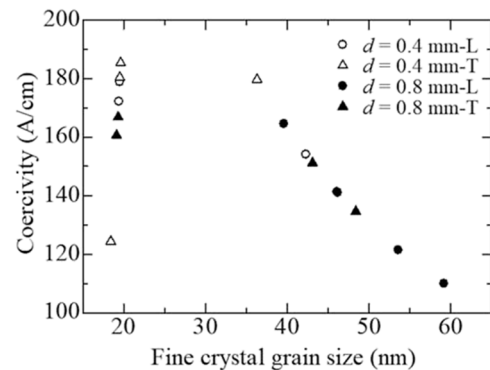


FIG. 4. Relationship between fine crystal grain size and coercivity.

## 2. Dislocation

It is known that martensite phase has high dislocation density.<sup>14</sup> When dislocation interacts strongly with the domain wall, a relative equation between  $H_c$  and dislocation density is proposed as shown in the following equation.<sup>15</sup>

$$H_c = (0.40 \pm 0.05) \frac{\rho^{2/3} E_0^{4/3}}{\gamma^{1/3} L_x^{2/3}} \frac{1}{\mu_0 M_s \delta_W}. \quad (4)$$

where  $\rho$  is dislocation density,  $E_0$  is a constant,  $L_x$  is the finite extension of the domain wall along the  $x$  axis,  $\delta_W$  is the Bloch wall thickness, and  $\gamma$  is domain wall energy. The  $H_c$  increases as the  $2/3$  power of the dislocation density from Eq. (4). The dislocation density of the martensite particle in SUS304 has a high value from the generation stage and displays a near linear increase with applied strain.<sup>14</sup> Therefore, the dislocation density as well as the  $H_c$  in the martensite phase increases with increasing  $V_f$ . As the material parameters except for the dislocation density are unknown, the number of times the  $H_c$  can change was evaluated by changing only the dislocation density. Further, as  $\rho = 5.04 \times 10^{14} \text{ m}^{-2}$  at strain  $\varepsilon$  of 0.2 and  $\rho = 5.39 \times 10^{14} \text{ m}^{-2}$  at strain  $\varepsilon$  of 0.8,<sup>14</sup> the relative equation between the dislocation density and strain  $\varepsilon$  is  $\rho = (5.83 \times 10^{13} \times \varepsilon + 4.92 \times 10^{14}) \text{ m}^{-2}$ . When  $\rho$  values at a plastic strain of 0.16 and again at 0.13 are calculated using the equation above,  $(\rho \text{ at plastic strain of } 0.16)^{2/3} / (\rho \text{ at plastic strain of } 0.13)^{2/3} = 1.002$ . Because this value corresponds to the ratio of the  $H_c$  at plastic strain of 0.13 and 0.16, the  $H_c$  of Specimen D4 increases 0.40 A/cm when the plastic stain increases from 0.13 to 0.16. In the experimental data, however, the  $H_c$  of Specimen D4 increased 6.7 A/cm and the analysis value was 0.06 times smaller than the experimental value. Moreover, in the case of A533B steel,<sup>16</sup> the  $H_c$  at the dislocation density of  $7 \times 10^{14} \text{ m}^{-2}$  is 8 A/cm and is two orders of magnitude smaller than the result. Therefore, we concluded that the dislocation is unlikely to be a controlling factor of  $H_c$ .

## 3. Shape anisotropy

Because martensite particles in the early stages of the martensite transformation are very small, they have a single lath structure<sup>17</sup> and could be potentially organized via rotation magnetization. As a result, the  $H_c$  of the martensite particle is affected by its shape anisotropy. The  $H_c$  was calculated by Eq. (5) of the Stoner-Wohlfarth model<sup>18</sup> to evaluate this effect. Assuming the particle shape to be prolate spheroid, the aspect ratio to be 1.05, and a random orientation as a result of an early stage of the martensite transformation, the  $H_c$  was calculated to be 113 A/cm. When the aspect ratio was raised to 1.1 in consideration of martensite particle growth, the  $H_c$  was calculated to be 220 A/cm, which is close to the experimental value.

$$H_c = 0.479(N_b - N_a)M_s. \quad (5)$$

where  $N_a$  and  $N_b$  are the demagnetization factor of the L and S axes of the martensite particle.

## B. Effects of grain size for susceptibility

In this section, the degree of influence on  $\chi$  of the fine grain size is evaluated using  $D$  calculated by Eqs. (3) and (6)<sup>4</sup> of initial

permeability  $\mu_i$ .

$$\mu_i = p_\mu \frac{\mu_0 M_s^2 A^3}{K_1^4 D^6}, \quad L_{ex} < D. \quad (6)$$

where,  $p_\mu = 0.33$  which is a material parameter.<sup>4</sup> In the case of  $V_f = 0.022\%$  of Specimen D4,  $\mu_i$  was calculated to be 15. As the  $\chi_0$  value obtained by this experiment at  $V_f = 0.022\%$  of Specimen D4 was 12.6, the converted permeability of 13.6 is considered a close match to the analytic value. However, when the  $\mu_i$  was calculated using the  $D$  of  $V_f = 0.041\%$ , the value was 14, which decreased, unlike the experimental result. In the previous paper,<sup>2</sup> the variance of the permeability along the L-axis increased by approximately 20% when the orientation angle, which is the angle from the L-axis, changed from 45 degrees to 40 degrees. In the experimental study, the  $\chi_0^L$  value increased approximately 47% when  $V_f = 0.020\%$  increased to  $V_f = 0.040\%$ . Taking into consideration the effects of aspect ratio,<sup>1</sup> the observed increase was sufficiently reasonable. The previous study<sup>2</sup> further explains that the orientation angle affected the permeability in the L and S axes via the effective magnetic field; the variance of permeability along the L-axis increased whereas that along the S-axis decreased with decreasing orientation angle. Hence, it is confirmed that the orientation angle generated a significant difference in the  $\chi$  and  $H_c$  in the L and S axes. The difference in the  $H_c$  and  $\chi$  between the Specimen D4 and the Specimen D8 will be discussed in the future because they have multiple causes.

## V. CONCLUSION

In this study, the magnetization curve along the long and short axes of type 304 stainless steel wires was measured and the coercivity and susceptibility of a single martensite particle were evaluated. The coercivity values along the long and short axes were measured to be greater than 100 A/cm, which increased and subsequently decreased with increasing martensite fraction. As mentioned in the above discussion, a martensite particle can be considered as a single domain structure during the early stages of the martensite transformation. Thus, it is expected that the coercivity and susceptibility parameters depend on the shape anisotropy of martensite particle. As the martensite transformation proceeds and particle size becomes larger, the size effects of variant clusters in a martensite particle begin to assume an important role in determining its coercivity and susceptibility. The excitation direction dependence of the susceptibility and coercivity are also affected by the orientation and aspect ratio of the particle.

## ACKNOWLEDGMENTS

The magnetic properties were measured on a Quantum Design MPMS-5S system in Research Center for Low Temperature and Materials Sciences, Kyoto University. I would like to express my sincere thanks to Assoc. Prof. Otsuka of Research Center for Low Temperature and Materials Sciences, Kyoto University and Assoc. Prof. Michioka of faculty of science, Kyoto University for their advice on using MPMS. I would also like to express my appreciation to Mr. Moriyama and Mr. Nakanishi, who are master's students at Kyoto University, for their help with Helium transfers. This work was supported by JSPS KAKENHI Grant Number 16K06386.

## REFERENCES

- <sup>1</sup>K. Kinoshita, R. Nakazaki, and E. Matsumoto, "Variation of the magnetic properties of the martensite phase of SUS304 steel due to tensile deformation," *Int. J. App. Electromagn. Mech.* **45**, 45 (2014).
- <sup>2</sup>K. Kinoshita, "Refinement of the magnetic composite model of type 304 stainless steel by considering misoriented ferromagnetic martensite particles," *AIP Adv.* **7**, 056008 (2017).
- <sup>3</sup>K. Miura, S. Kobayashi, Y. Kamada, Y. Onuki, and J. A. Szipunar, "Relationship between morphology of strain-induced martensite phase and magnetic properties in austenitic stainless steels," *J. Jpn. Inst. Met. Mater.* **78**, 375 (2014).
- <sup>4</sup>G. Herzer, "Grain size dependence of coercivity and permeability in nanocrystalline ferromagnet," *IEEE Trans. Magn.* **26**, 1397 (1990).
- <sup>5</sup>G. B. Olson and M. Cohen, "Kinetics of strain-induced martensitic nucleation," *Metall. Trans.* **6A**, 791 (1975).
- <sup>6</sup>T. Fukumaru, H. Hidaka, T. Tsuchiyama, and S. Takagi, "Effect of wire diameter and grain size on tensile properties of austenitic stainless steel wire," *Tetsu-to-Hagané* **91**, 828 (2005), in Japanese.
- <sup>7</sup>P. Merinov, S. Entin, B. Beketov, and A. Runov, "The magnetic testing of the ferrite content of austenitic stainless steel weld metal," *NDT international* **11**, 9 (1978).
- <sup>8</sup>A. K. Mumtaz, S. Takahashi, J. Echigoya, Y. Kamada, L. Zhang, H. Kikuchi, K. Ara, and M. Sato, "Magnetic measurements of the reverse martensite to austenite transformation in a rolled austenitic stainless steel," *J. Mat. Sci.* **39**, 1997 (2004).
- <sup>9</sup>F. Sato, N. Tezuka, T. Sakurai, and T. Miyazaki, "Grain diameter and coercivity of Fe, Ni, and Co metals," *IEEE Transl. J. Magn. Jpn.* **9**, 100 (1994).
- <sup>10</sup>G. Herzer, *Handbook of magnetic materials* (Elsevier B.V., 1997), Chap. 3, p. 415.
- <sup>11</sup>Q. Zeng, I. Baker, V. McCreary, and Z. Yan, "Soft ferromagnetism in nanostructured mechanical alloying FeCo-based powders," *J. Magn. mag. Mater.* **318**, 28 (2007).
- <sup>12</sup>A. Shibata, M. Chen, A. Matsumoto, M. Tsuboi, T. Miyazawa, M. Sato, and N. Tsuji, "Stress-induced martensitic transformation behavior analyzed by in-situ measurement of local stress field under elastic deformation," [https://support.spring8.or.jp/Report\\_JSR/PDF\\_JSR\\_26A/2014A1578.pdf](https://support.spring8.or.jp/Report_JSR/PDF_JSR_26A/2014A1578.pdf) (2014).
- <sup>13</sup>Y. Murata, "Formation mechanism of lath martensite in steels," *J. Japan Inst. Met. Mater.* **80**, 669 (2016).
- <sup>14</sup>T. Shintani and Y. Murata, "Evaluation of the dislocation density and dislocation character in cold rolled type 304 steel determined by profile analysis of X-ray diffraction," *Acta. Mater.* **59**, 4314 (2011).
- <sup>15</sup>H. R. Hilzinger, "Computer simulation of magnetic domain wall pinning," *Phys. Stat. sol. (a)* **38**, 487 (1976).
- <sup>16</sup>S. Takahashi, J. Echigoya, and Z. Motoki, "Magnetization curves of plastically deformed Fe metals and alloys," *J. Appl. Phys.* **87**, 805 (2000).
- <sup>17</sup>M. Chen, D. Terada, A. Shibata, and N. Tsuji, "Identical area observations of deformation-induced martensitic transformation in SUS304 austenitic stainless steel," *Mater. Trans.* **54**, 308 (2013).
- <sup>18</sup>K. Oota, *Jikikogakunokiso ii* (Kyoritsu Shuppan, 1973), pp. 287–295.